

# A network compression approach for quantifying the importance of temporal contact chronology

Andrea J. Allen,<sup>1</sup> Cristopher Moore,<sup>2</sup> and Laurent Hébert-Dufresne<sup>1,3</sup>

<sup>1</sup>Vermont Complex Systems Center, University of Vermont, Burlington VT

<sup>2</sup>Santa Fe Institute, Santa Fe, NM 87501, USA

<sup>3</sup>Department of Computer Science, University of Vermont, Burlington VT

Studies of dynamics on temporal networks often look at the overall impact of temporal structural changes, falling back on static networks when the changes are slow, or on average annealed networks when the changes are fast. In between these limits, we propose a method to quantify the importance of chronology in temporal network data by using an epidemic spreading approach and looking at the commutative property of consecutive snapshots. We use this method to reduce the number of snapshots in real sequences of contact data by algorithmically compressing consecutive snapshots. We find that the framework succeeds in mimicking the fully temporal dynamics, and can also be used to assess the sensitivity of the data to temporal variations.

**Introduction** Modern data collection methods such as radio frequency identification [1] or Bluetooth signal [2] have made the collection of high resolution temporal interaction data simple and widely available. Temporal interactions have rich dynamics in continuous time, yet we often want to combine intervals of temporal data into simpler, aggregate structures in order to compress the data themselves, reduce analytical complexity, or even to streamline data collection efforts. For example, digital contact tracing protocols ping devices at fixed intervals to save energy and lighten data requirements. However, it is nontrivial to determine when and how to aggregate temporal data without losing critical information about the dynamics of the interactions.

Many methods currently exist to represent and analyze temporal networks [3]. Much recent work focuses on simplifying temporal networks through patterns in the network structure and dynamics; providing algorithms for detecting temporal system states [4], dynamical approach for generating simplified models of temporal network data [5], tools to identify community structure in time-varying networks [6], data-driven approaches to model dynamics on temporal networks by determining change points [7], and methods to represent key temporal features as static networks [8, 9]. Purely from a dynamical perspective, epidemic spread on temporal networks is well-studied [10–13], as are synchronization [14–16] and control dynamics [17].

Taken together, these previous studies outline the limits in which one can put aside chronology in network structure. When the dynamics *on* the network are much faster than the dynamics *of* the network, the static limit of the network is appropriate, in which many dynamical steps of the network structure can be combined to yield the same behavior of the dynamics on the network. When the dynamics on the network are much slower than the network changes, then it is safe to average over many timesteps, referred to as the annealed limit. In both limits, the dynamical history of the network can be compressed in a clear way. In between these limits, it is less clear to what extent the temporal history of the network structure can be compressed while remaining faithful to the dynamics on the network. Here, we address the problem of quantifying if a sequence of networks lies in between these two limits; thereby allowing us to ignore and compress unim-

portant structural changes while preserving changes that affect the dynamical process.

We propose a novel method for quantifying the importance of chronological dynamics in temporal data by assessing the sensitivity of pairwise network snapshots to aggregation. We consider an epidemic spreading process but abstract the dynamics to a simple diffusion process which could represent other dynamical processes on networks (e.g., synchronization of coupled oscillators or cascading failures in power grids) and formulate a pair-wise error measure that signifies the effects on the diffusion process of aggregating snapshots into a static network. We use the error measure to successively compress a sequence of chronological snapshots by compressing the adjacent pair of snapshots with the lowest relative error. Using synthetic networks and real data, we find that this approach is successful at producing a compressed snapshot sequence that still mimics the dynamic behavior of the original sequence.

**Analytical framework** We assume that we have some temporal network data consisting of a large number of snapshots of the network structure. This comes without loss of generality as even continuous time data could be represented

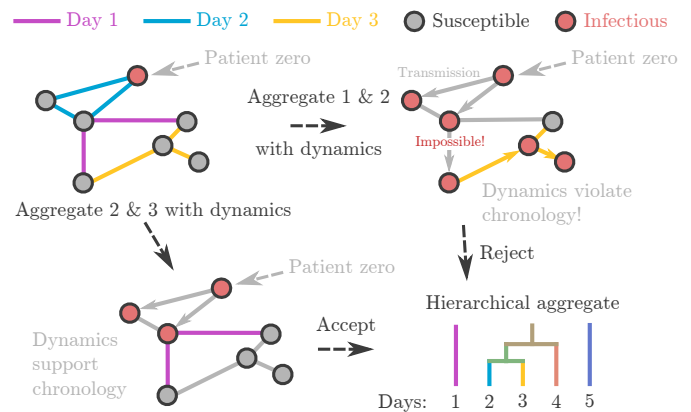


FIG. 1: Schema of our hierarchical aggregation. Given network snapshots, we compare the aggregate spreading dynamics of each adjacent pair of snapshots and combine the pair with the lowest induced error, continuing until we reach a desired number of snapshots.

as a large series of mostly empty graphs. We then wish to quantify the importance of temporal chronology by measuring the error we would introduce by combining any two consecutive networks into a single aggregated, static, snapshot. From there, we can simply compress aggregations that minimize this error (Fig. 1).

To this end, we study an epidemic diffusion process on a sequence of two successive networks. We assume the contagion spreads at a rate  $\beta$  along edges connecting infectious nodes to their susceptible neighbors. We ignore recovery events, assuming that they occur at a much slower timescale than the temporal resolution of our data. We measure the effect of pairwise aggregation by observing the difference in size of the infected compartments under the temporal and aggregate regimes over the duration of the snapshot pair.

**Snapshot definitions** Let  $X = [X_{ij}]$  be the adjacency matrix for a static network. Assume  $X$  is valid for a duration  $\delta t_X = t_1^X - t_0^X$ , the  $t_1^X$  and  $t_0^X$  are the ending and starting times of  $X$ , and transmission of a spreading process occurs between contacts with rate  $\beta_X$ . Then we call  $(X, \delta t_X, \beta_X)$  a snapshot.

Assume  $(X, \delta t_X, \beta)$  and  $(Y, \delta t_Y, \beta)$  are snapshots such that  $\delta t_Y = t_1^Y - t_0^Y$  and  $t_0^Y = t_1^X$ , with a uniform  $\beta$ . Then  $X$  and  $Y$  are consecutive snapshots. Given snapshots  $(X, \delta t_X, \beta)$  and  $(Y, \delta t_Y, \beta)$ , let the aggregate  $(\overline{X, Y})$  with respect to  $(\delta t_X, \delta t_Y)$  be

$$\overline{(X, Y)} = \frac{\delta t_X X + \delta t_Y Y}{\delta t_X + \delta t_Y}. \quad (1)$$

**Solution of diffusion on a network** Let  $A$  be the adjacency matrix of a network with  $N$  nodes. Let  $P(t)$  be a vector of length  $N$  encoding the probability that each of the nodes from node 0 to node  $N - 1$  is infected at time  $t$ . Then the rate of change of  $P(t)$  is given by the following differential equation:

$$\frac{dP}{dt} = \{1 - P(t)\}\beta AP(t) - \alpha P(t) \quad (2)$$

where from here forward we will drop the term  $\alpha P_i$  since we set  $\alpha = 0$  in this  $SI$  model, either because there is no recovery in the system or because it happens on a much slower timescale than contagion and/or network dynamics. We can solve for a close approximation of  $P(t)$ , and then compute the size of the infected compartment as  $I(t) = |P(t)|$ .

**Approximation of diffusion** If we assume large  $N$  and early time  $t$  such that infections are rare enough to approximate  $(1 - P(t)) \approx 1$ , the solution for the entire system with all nodes can be written by the following differential equation that utilizes the matrix exponential

$$P(t) = \exp \beta A t \cdot P(0) \quad (3)$$

where  $P(0)$  is vector of initial probabilities of infection for each node. We assume the initial state of each system of snapshot pairs follows the expected dynamics of the first snapshot during the course of an ongoing spreading process. To do so, we simply set  $P(0) \propto [k_0, k_1, k_2, \dots, k_{N-1}]$  where each  $k_i$  is the degree of node  $i$  from 0 to  $N - 1$ , normalized such that  $\sum P(0) = 1$  to represent a single patient zero without loss of generality.

Say we have two consecutive snapshots,  $(A, \delta t_A, \beta)$  and  $(B, \delta t_B, \beta)$ . We define the operator  $T(A)$  as the transmission dynamics on the snapshot, written as

$$T(A) = \beta \delta t_A A. \quad (4)$$

We consider two regimes of dynamics on the pair of snapshots: temporal, where we switch from  $A$  to  $B$  at the switch-point time  $t_1^A = t_0^B$ , and aggregate, where we consider  $(\overline{A, B})$  for the full duration  $t : [t_0^A, t_1^B]$ .

Under the matrix approximation respecting the chronology of the two consecutive snapshots, the solution at the end of the duration of the two snapshots is given by

$$P(t_1^B) = \exp \{T(B)\} \cdot \exp \{T(A)\} \cdot P(0), \quad (5)$$

and in the case where we aggregate the pair of snapshots,

$$P(t_1^B) = \exp \{T(\overline{A+B})\} \cdot P(0), \quad (6)$$

where  $T(\overline{A+B}) = \beta(\overline{A+B})(\delta t_A + \delta t_B) = \beta(\delta t_A A + \delta t_B B) = T(A) + T(B)$ , following from Eq. (1). It is important to note that unless  $A$  and  $B$  are commutative, Eq. 5 and Eq. 6 are not equal, as demonstrated in Fig. 2. If two snapshots  $A$  and  $B$  are commutative, then mathematically, the diffusion solution applies the dynamics on these two snapshots simultaneously, since using the aggregate  $\overline{A+B}$  is identical to using  $A$  and  $B$  in any sequence. Therefore, assessing the ability for two snapshot matrices to commute is a practical way to infer if their chronology is important to the diffusion dynamics.

**Aggregation error** When two matrices  $X$  and  $Y$  do not commute, the Baker-Campbell-Hausdorff formula can express the product  $\exp(Y)\exp(X)$  as a single exponential where we define the matrix  $Z$  as

$$Z = \log(\exp Y \exp X) = Y + X + \frac{1}{2} [Y, X] + \frac{1}{12} \{[Y, [Y, X]] + [X, [X, Y]]\} + \dots \quad (7)$$

in which  $[Y, X] = YX - XY$ , the commutator of  $X$  and  $Y$ . The commutator captures the sensitivity of the temporal ordering of  $X$  and  $Y$ . Letting the matrix  $C = \log(\exp T(B)\exp T(A))$ , and using the Baker-Campbell-Hausdorff equation,  $C$  can be expressed as

$$C \simeq T(B) + T(A) + \frac{1}{2} \{T(BA) - T(AB)\} + \frac{1}{12} \{T(BBA) + T(ABB) + T(AAB) + T(BAA)\} - \frac{1}{6} \{T(BAB) + T(ABA)\}, \quad (8)$$

where we approximate by using matrix products up to third order, as higher order terms scale with  $\tau^n$  and thus fall to zero rapidly for  $n > 3$ . We solve for  $\exp(C)$  by using the Taylor series expansion definition, again up to terms in  $\tau^3$ .

To quantify the expected difference between the sizes of infected compartments following Equation (8) for the temporal

regime, we take the definition of the matrix exponential up to order three to match terms in Eq. (8) and evaluate

$$\epsilon_{END} = \sum_{i=0}^{N-1} \left\{ \exp(C) - \exp(T(A+B)) \right\} P(0). \quad (9)$$

Letting  $D$  be the difference matrix shorthand between the temporal and aggregate matrices above, we compute  $D = \exp(C) - \exp(T(A+B))$  as

$$D = \frac{1}{2} \{T(BA) - T(AB)\} + \frac{1}{3} \{T(BBA) + T(BAA)\} \\ - \frac{1}{6} \{T(BAB) + T(ABA) + T(ABB) + T(AAB)\} \quad (10)$$

Recall that a product  $BA$  can be interpreted as a path of length two where the first step is done in  $A$  and the second in  $B$ . Equation (10) captures paths that switch snapshots, but follow the chronology (positive terms), and also paths that violate the chronology of the two snapshots (negative terms). Paths that violate chronology are accounted for by any term that involves the matrix product  $AB$ . For example, if a contact between nodes 1 and 2 occurs in snapshot  $A$  before a contact between 2 and 3 in snapshot  $B$ , then a disease could spread from node 1 to 3; if these contacts occur in the opposite order, however, then this two-step transmission path cannot occur. Since  $\exp(A+B) = \exp(B)\exp(A)$  to first order, the higher-order terms kept in our calculations form the main contributions to the corrective term.

Now using Eq. (10) to solve for Eq. (9), we summarize the error induced as

$$\epsilon_{END} = \sum_{i=0}^{N-1} [|D_{ij}|] \cdot P(0), \quad (11)$$

an approximation for the total difference between the sizes of the infected compartments after  $t$  time under the temporal and aggregate regimes, where we take the element-wise absolute value of each entry to account for time-violating transmissions that either under- or over-estimate the number of infections.

However, even if the terminal error is zero (or negligible), we can see why in Fig. 2 the dynamics of the spreading process may still behave dramatically differently under the temporal and aggregate regimes. To account for this, we also approximate the error at the midpoint, that is,  $\delta t_A$ . This version of the difference matrix approximation truncated to terms of order 3 is given by

$$D = \sum_{n=1}^3 \frac{(\beta \delta t_A A)^n - (\beta \delta t_A \overline{A+B})^n}{n!} \quad (12)$$

and we find  $\epsilon_{MID}$  the same way by taking  $\epsilon_{MID} = \sum_{i=0}^{N-1} [|D_{ij}|] \cdot P(0)$ .

Finally, we define the error  $\xi_{A,B}$  as the approximated contributed effect of aggregating snapshots  $A$  and  $B$  on a spreading process with spreading rate  $\beta$  over the durations 0 to  $\delta t_A$

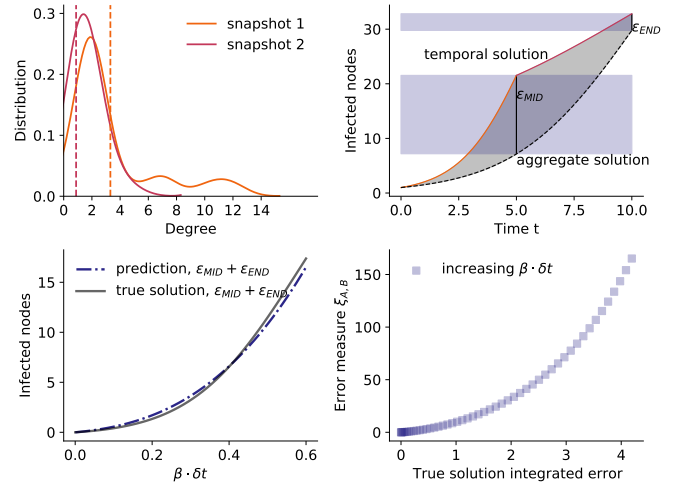


FIG. 2: Top left: Degree distributions for two example snapshots. Top right: Deterministic solutions of an  $SI$  spreading process with  $\beta = .12$ ,  $\delta t = 5$  on the temporal and aggregate versions of the snapshots, with indicator labels for  $\epsilon_{MID}$  and  $\epsilon_{END}$ . Bottom left: True solution and predicted difference in number of infected nodes under the temporal and aggregate regimes for varying values of  $\tau = \beta t$  by varying  $t = [0, 5]$ . Bottom right: the error measure  $\xi_{A,B}$  for snapshots  $A$  (snapshot 1) and  $B$  (snapshot 2) is monotonic with respect to the solution of the integrated area between the temporal and aggregate curves, as shown in the top right.

to  $\delta t_B$ , defined as

$$\xi_{A,B} = (\epsilon_{END} + \epsilon_{MID})(\delta t_A + \delta t_B). \quad (13)$$

Eq. (13) can be justified as follows. To measure the error induced by aggregating the snapshots  $A$  and  $B$ , we ideally want to estimate the shaded area between the curves as in Fig. (2). Eq. (13), while providing a crude estimate, preserves the ranking of pairs from least to most induced error when computed over all possible pairs  $A, B$ . As such,  $\xi_{A,B}$  is useful less so for perfect error estimation, but as a tool for selecting the pair with the least induced error.

We want to highlight that  $\xi_{A,B}$  vanishes for the base case in which  $T(B) = T(A)$ . All terms in Eq. (10) and Eq. (12) cancel out, since for any step in one network exists an equivalent step in the other network, and therefore the positive and negative terms sum to zero. When  $T(B)T(A) = 0$ , all terms in Eq. (10) are directly zero since there exist no path that can go from one network to the other, however the switchpoint error Eq. (12) may be nonzero.

**Compression Algorithm** Given a set of temporal data as a sequence of  $M$  snapshots, we can use the framework to compress the snapshots into  $M - j$  snapshots via a greedy algorithm. First, the number of desired iterations  $j$  is set. For steps from 1 to  $j$ ,

1. The error  $\xi_{A,B}$  from Eq. (13) is computed for each pair  $A, B$  of ordered, consecutive snapshots.
2. Identify the pair  $A^*, B^* = \operatorname{argmin}_{A,B}(\xi_{A,B})$  to be com-

pressed.

3. Replace snapshots  $(A, \delta t_A, \beta)$  and  $(B, \delta t_B, \beta)$  with their aggregate,  $(A + B, \delta t_A + \delta t_B, \beta)$ .

**Results** The proposed aggregation algorithm produces a set of temporal snapshots that are able to better support the spreading dynamics of the fully temporal network than the set of evenly divided and compressed snapshots. To assess the performance of the compression algorithm against an evenly distributed compression, we integrate the dynamics of Eq. (2) over the full temporal set of snapshots,  $x(t)_{TEMP}$ , as well as over the system defined by the new sets of even snapshots,  $x(t)_{EVEN}$ , and the snapshots produced by the algorithm,  $x(t)_{ALG}$ . We define a validation error measure  $d_{EVEN}$  (and  $d_{ALG}$ , respectively) as

$$d_{EVEN} = \int \frac{|x(t)_{EVEN} - x(t)_{TEMP}|}{x(t)_{TEMP}} dt \quad (14)$$

with  $d_{ALG}$  defined analogously. We apply the algorithm to synthetic networks in Fig. 3 and real data in Fig. 4.

The error metric defined in Eq. (13) picks up on the sensitivity of pairs of snapshots to aggregation, and can be assessed at any level of snapshot resolution. We show in the top panel of Fig. 4 how the sensitivity of certain temporal ranges is maintained over a large range of resolution, which allows for pre-aggregation of data to improve the speed of the algorithm. Importantly, the error metric allows us to identify the daily patterns of the contact data at a glance. Once integrated in the compression algorithm, the middle panel shows how we can aggregate over nights and capture the daily activity in one or two snapshots. As seen in the bottom panel, our algorithm compresses more than twice as much as evenly distributed compression while retaining a given level of error on the resulting dynamics.

**Discussion** The error term  $\xi$  obtained in Eq. (13) is a fast approach to estimating aggregation error using the matrix exponential. There are four interesting applications for the  $\xi$  error term. First, it can directly provide bounds of accuracy when studying dynamics on temporal networks with tools developed for epidemics on static networks. Our analytical error estimate starts with a description of epidemic dynamics but was boiled down to a simple diffusion rate. While other mechanisms (saturation and recovery) were ignored, Fig. 2 showed how accurate our approach remained. Consequently, our tool could very likely be used to estimate error around other type of diffusion dynamics.

Second, it can help compress large sequences of temporal networks by combining any consecutive pair of network  $T(A)$  and  $T(B)$  into an aggregate if the expected error on the aggregate is smaller than some threshold. We can apply this process recursively and hierarchically to compress the data to a much smaller sequence of networks while keeping track of the duration of each network snapshot. As shown in Fig. 4 using real temporal interaction data, this approach allowed us to consistently meet a certain level error while decreasing the number of required network snapshots by a factor of almost 2.

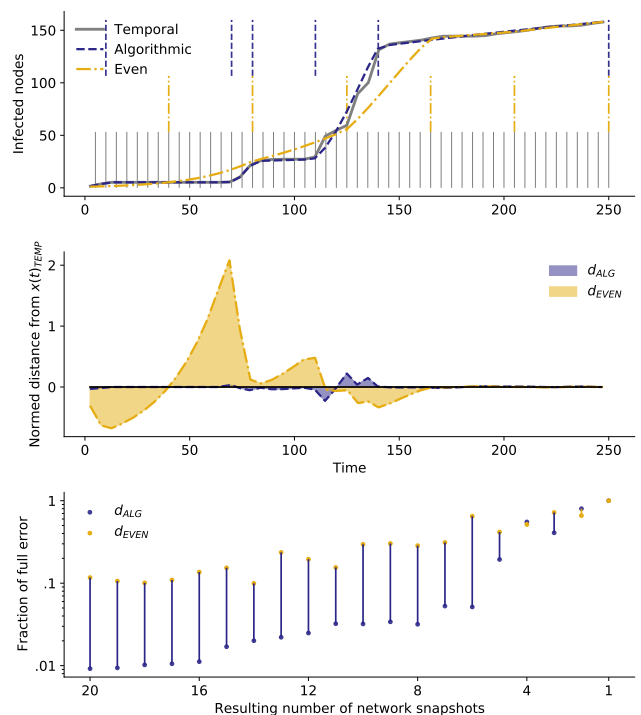


FIG. 3: Compression algorithm run on a series of 50 synthetic network snapshots into 6 aggregate snapshots, with a  $\beta = .0017$  and intervals of  $t = 5$  such that  $\beta\delta t \in [.0085, .42]$ . Blue dashed lines represent the boundaries for the resulting snapshots from our algorithm, yellow represent the boundaries for the evenly distributed aggregated snapshots. Middle panel shows the normalized distance from the temporal curve over time for each solution. Bottom panel shows the sum of the shaded area in the middle panel as a function of resulting number of aggregated snapshots, relative to the error induced by the full aggregation.

Third, the error can be used to estimate the accuracy of data collection in the first place by testing how compressible it could be. This might help focus data collection efforts by identifying places and times with fast temporal variations, as in the top panel of Fig. 4. Fourth, the error can be used on non-temporal data to compare the structure of any two networks  $T(A)$  and  $T(B)$  that share some of the same nodes. At its core, our approach is a network comparison tool: How different are networks when compared to their average?

Limitations of the method include its sensitivity to spreading process parameters to keep  $\beta\delta t$  within the appropriate range for the matrix exponential approximation, requiring the dynamics to be slow compared to the timescale of network snapshots. Another limitation is the greediness of the algorithm, which means it can get stuck in sub-optimal compression sequence when compressing a long sequence to a handful of snapshots. Future work might explore how to better predict the optimal stopping point of temporal compression.

Altogether, we hope that our work will inspire more tools to compress temporal network data which is an area rich in possible applications.

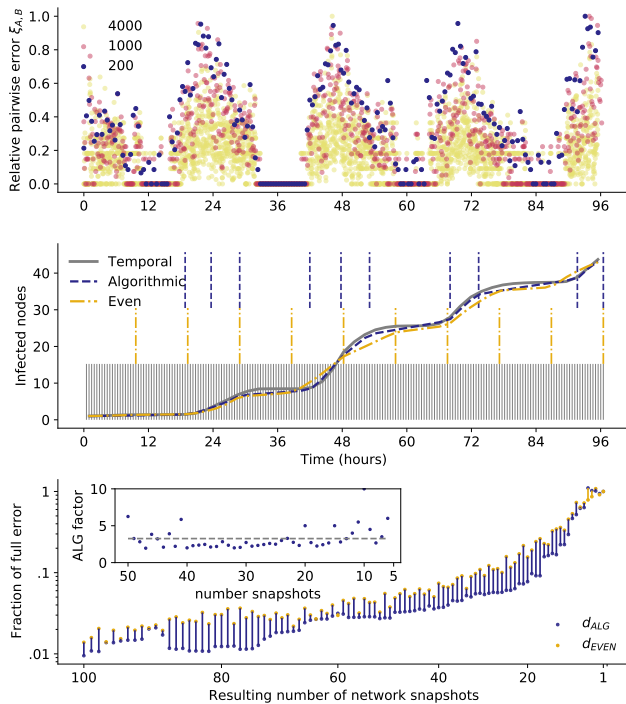


FIG. 4: Application to a hospital contact network [18]. Top panel: the error measure  $\xi_{S(t),S(t+1)}$  computed for consecutive snapshot ( $S$ ) pairs at 3 different levels of pre-aggregation. The hospital contact dataset contains contacts for approximately 9,000 unique timestamps. We pre-aggregate by evenly coarse-graining the data to 4,000, 1,000 and 200 snapshots. Mid panel: the compression algorithm run on a the 200 snapshots to generate 10 snapshots, compared to the fully temporal dynamics and the dynamics under even compression. The pre-aggregated 200 snapshots each have duration 1737 seconds with mean 27.34 contacts per snapshot. We used a  $\beta = .000015$  such that  $\tau \in [0.025, 0.5]$ . Vertical lines show boundaries for the resulting aggregated snapshots. Bottom panel shows the sum of the shaded area in middle panel function of resulting number of aggregated snapshots, relative to the error induced by the full aggregation. The inset shows by what factor our algorithm can further compress the snapshot sequence while producing an error less than the even aggregation at the number of snapshots shown.

**Acknowledgements** The authors acknowledge support from the National Institutes of Health 1P20 GM125498-01

Centers of Biomedical Research Excellence Award and the National Science Foundation Grant No. DMS-1829826.

- 
- [1] C. Cattuto, W. Van den Broeck, A. Barrat, V. Colizza, J.-F. Pinton, and A. Vespignani, *PloS ONE* **5**, e11596 (2010).
  - [2] P. Sapiezynski, A. Stopczynski, D. D. Lassen, and S. Lehmann, *Scientific Data* **6**, 1 (2019).
  - [3] P. Holme and J. Saramäki, *Physics Reports* **519**, 97 (2012).
  - [4] N. Masuda and P. Holme, *Scientific Reports* **9**, 795 (2019).
  - [5] T. P. Peixoto and M. Rosvall, *Nature Communications* **8**, 582 (2017), place: England Publisher: Nature Publishing Group UK.
  - [6] A. Ghasemian, P. Zhang, A. Clauset, C. Moore, and L. Peel, *Physical Review X* **6**, 031005 (2016), publisher: American Physical Society.
  - [7] T. P. Peixoto and L. Gauvin, *Scientific Reports* **8**, 15511 (2018).
  - [8] P. Holme, *PLoS Computational Biology* **9** (2013), <https://doi.org/10.1371/journal.pcbi.1003142>.
  - [9] I. Scholtes, N. Wider, and A. Garas, *The European Physical Journal B* **89**, 61 (2016).
  - [10] L. E. C. Rocha, F. Liljeros, and P. Holme, *PLoS Computational Biology* **7** (2011), <https://doi.org/10.1371/journal.pcbi.1001109>.
  - [11] M. Génois, C. L. Vestergaard, C. Cattuto, and A. Barrat, *Nature Communications* **6**, 8860 (2015).
  - [12] G. Ren and X. Wang, *Chaos* **24**, 023116 (2014), publisher: American Institute of Physics.
  - [13] E. Valdano, L. Ferreri, C. Poletto, and V. Colizza, *Physical Review X* **5**, 021005 (2015), publisher: American Physical Society.
  - [14] S. Boccaletti, D.-U. Hwang, M. Chavez, A. Amann, J. Kurths, and L. M. Pecora, *Physical Review E* **74**, 016102 (2006).
  - [15] D. J. Stilwell, E. M. Bollt, and D. G. Roberson, *SIAM Journal on Applied Dynamical Systems* **5**, 140 (2006).
  - [16] Y. Zhang and S. H. Strogatz, *Nature communications* **12**, 1 (2021).
  - [17] A. Li, S. P. Cornelius, Y.-Y. Liu, L. Wang, and A.-L. Barabási, *Science* **358**, 1042 (2017).
  - [18] P. Vanhems, A. Barrat, C. Cattuto, J.-F. Pinton, N. Khanafer, C. Régis, B.-a. Kim, B. Comte, and N. Voirin, *PLoS ONE* **8**, e73970 (2013), publisher: Public Library of Science.